Sustainable Removal of Crystal Violet Dye Using Synthesized Albizia Procera-Iron Activated Carbon Nanoparticles (AP-Fe-Ac Nps) : Kinetics, Isotherms and Thermodynamics

Kapavarapu Sreekar[1], *Beeram* Sri Mahi Saroj Prathap[1], *Yagna* Sri Thikkada[1*], *Kethineedi* Vyshnavi[1], *Pichika* Satya Kedarnath[2], and *Meena* V[3]

[1]Btech Student, Department of Chemical Engineering, AUCE, Andhra University, Ap, India.
[2]Senior Engineer Operations, Gail(India)Limited, India.
[3]Professor, Department of Chemical Engineering, AUCE, Andhra University, Ap, India.

Abstract. In present era, green synthesis methodologies showcases the liabilities in synthetization of nanoparticles and elimination of stains using this synthesized nanoparticles because of their less influencing environmental toxicity. Alblizia procera leaf extract is used in this present studies as it is a promising capping and reducing agents like phenols and other attributed biomolecules, to synthesize FeNp's-AC in this experiment. The action of ferrous-activated carbon nano-sized particles is calibrated using FTIR, SEM and XRD methods. This experimentation is based on process called Adsorption in the extraction of crystal violet tint are carried out for different parameters which include: dosage, contact time, pH and temperatures were studied and optimized. The Freundlich, Langumir and Temkin Isotherm models for Crystal violet are proved to be the best adjustments for the AP-Fe-ACNp's experimental data.

1 Introduction

Dyes are colored compounds that exhibit a high affinity for special materials, such as textiles paper, leather, and plastics[1]. The affinity allows dyes to form strong chemical bonds with the fibers of the material, resulting in the imbuing of color. In contrast, pigments are insoluble particles that provide coloration through physical adsorption onto the surface of a material[2].

1.1 Crystal Violet

Crystal violet, also known hexamethyl pararosaniline chloride is a positively charged (cationic) triarylmethane dye. This molecular characteristic enables it to form strong ionic bonds with negatively charged biomolecules such as DNA and cell walls, rendering it a valuable tool in various biological research applications [3]. In microbiology, this property is leveraged in Gram staining, a fundamental technique for bacterial classification based on

* Corresponding Author: yagnathikkada1110@gmail.com

cell wall composition[4]. Gram-positive bacteria, possessing a thicker peptidoglycan layer, retain the stain-iodine complex in due course of staining, resulting in a characteristic purple color[5].

Crystal violet also offers a non-toxic alternative for DNA visualization in gel electrophoresis[6]. By binding to DNA fragments, it facilitates their visualization under white light, eliminating the need for mutagenic UV light employed by some other DNA staining techniques[7].

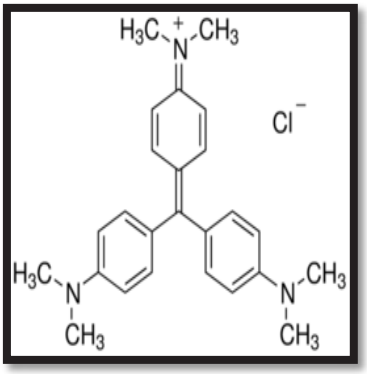

Fig. 1. Structure of Crystal Violet

1.2 Albizia Procera

The bark of Albizia procera, possesses a unique property: the ability to extract and remove dyes. When processed, this bark yields natural compounds that effectively interact with and neutralize a variety of dyes[8]. This characteristic has led to its historical application in the textile industry, where Albizia procera has facilitated colour removal during fabric dyeing processes[9]. Consequently, this seemingly ordinary tree may have played a significant role in achieving the vibrant colours we admire in many textiles.

Fig. 2. Albizia Procera

1.3 Ferrous Nanoparticles

Iron nanoparticles, incredibly tiny iron particles ranging from 1 to 100 nano meters, possess unique characterizations because of their miniature size[10]. Their vast surface bounded area makes them highly reactive, potentially attracting and binding to dye molecules[11]. This characteristic has researchers exploring their use in the textile industry for dye removal. Iron nanoparticles could potentially revolutionize wastewater treatment by capturing dyes from industrial effluents before they reach waterways[12]. Additionally, their magnetic properties, depending on their composition, might allow for easy separation using magnets, simplifying the dye removal process[13]. While research on their effectiveness and potential environmental impact is ongoing, iron nanoparticles offer a promising avenue for cleaner and more sustainable dye removal methods[14].

1.4 Activated Carbon Fe Nanoparticles

Activated carbon iron particles (AP-Fe-ACNps) combine the remarkable properties of activated carbon with the potential of iron nanoparticles for a powerful approach to dye removal. Activated carbon, a highly porous material with a vast surface area, is already widely used for its exceptional ability to adsorb various molecules, including dyes, from liquids. When iron nanoparticles are incorporated into activated carbon, they can further enhance dye removal through several mechanisms[15]. The iron nanoparticles can act as additional adsorption sites, attracting and binding to specific dye molecules through chemical interactions. Additionally, depending on the type of iron used, the particles might introduce magnetic properties to the AP-Fe-ACNps. This magnetism could allow for easier separation of the dye-laden AP-Fe-ACNps from the treated water using an external magnet, streamlining the dye removal process [16]. This combination offers a potentially cost-effective and efficient method for wastewater treatment, particularly for removing dyes from industrial effluents. As research continues to optimize AP-Fe-ACNps sign and explore their long-term environmental impact, they hold significant promise for a cleaner and more sustainable future in dye removal processes.

2 Materials and Methods

The Albizia procera leaves are gathered from the regional location.

2.1 Chemical Essentials:

Ferric(III) chloride($Fecl_3$), activated charcoal, HCl, NaOH.

2.2 Glassware:

1 litre bearing beaker, standard measuring jar, Pipette, conical flasks

2.3 Apparatus:

pH meter, mechanically operated stirrer, Spectrophotometer, Orbital Shaker and Glass materials etc.

2.4 Quantification of Crystal Violet

2.4.1 Tint Sample Composition:

1g of tint is diluted in 1000 ml water containing beaker, thus results in desired sample.

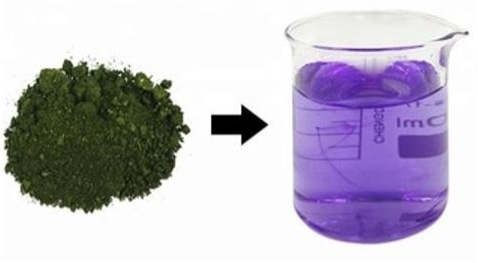

Crystal violet solution

Fig. 3. Crystal Violet Solution

2.5 Preparation of Albizia Procera Leaf Extract

Desired leaves are subjected to washing under laminar run flow of water and later screened with sterilization mechanism(water source: distilled water; purpose: removal of dust particles). The leaves are then dried in presence of sunlight to make them moist-free. These processed leaves are quantified to 10g , finely chopped and this is put in sterilized distilled water(200ml). this resultant mixture is subjected to boiling for a period of 10 mins till the solution Colour turns from watery to yellow and later cooled at room temperature. This final mixture is filtered with Whatman no.1 filtering paper and finally subjected to centrifugation process for about 10mins in order to pull out undesired biological materials.

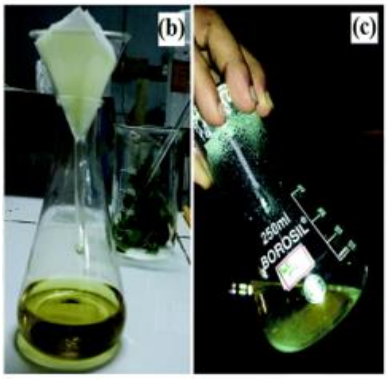

Fig. 4. Leaf Extract

2.6 Synthesis of iron nanoparticles(AP-Fe-ACNps):

Iron nanoparticles were synthesized by using albizia procera leaves extract by putting in $fecl_3$ to it. 8.11 grams of $FeCl_3$ granules taken in 500ml water measuring jar and add 1.25 grams of activated carbon. On precautionary note, the ratio must be in 1:1 to the resulted quantity

after the filter process of leaf extract. This quantified mixture is subjected to continuous stirring with the aid of mechanical stirrer at room temp. The rapid formation of black precipitate clearly indicates the presence of Fe^{+2} ions. This ,formed precipitate is subjected to centrifugal process (conditions- speed: 5000 rpm, period:20 mins). Gradually, the Fe nano-sized particles are desiccated to 65^0C in vaccum environment for approximately 3hrs.

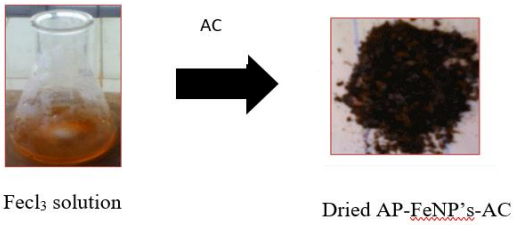

Fig. 5. AP-FeNP's-AC

2.6.1 Synthesis process for FeNP-AC (Flow Diagram)

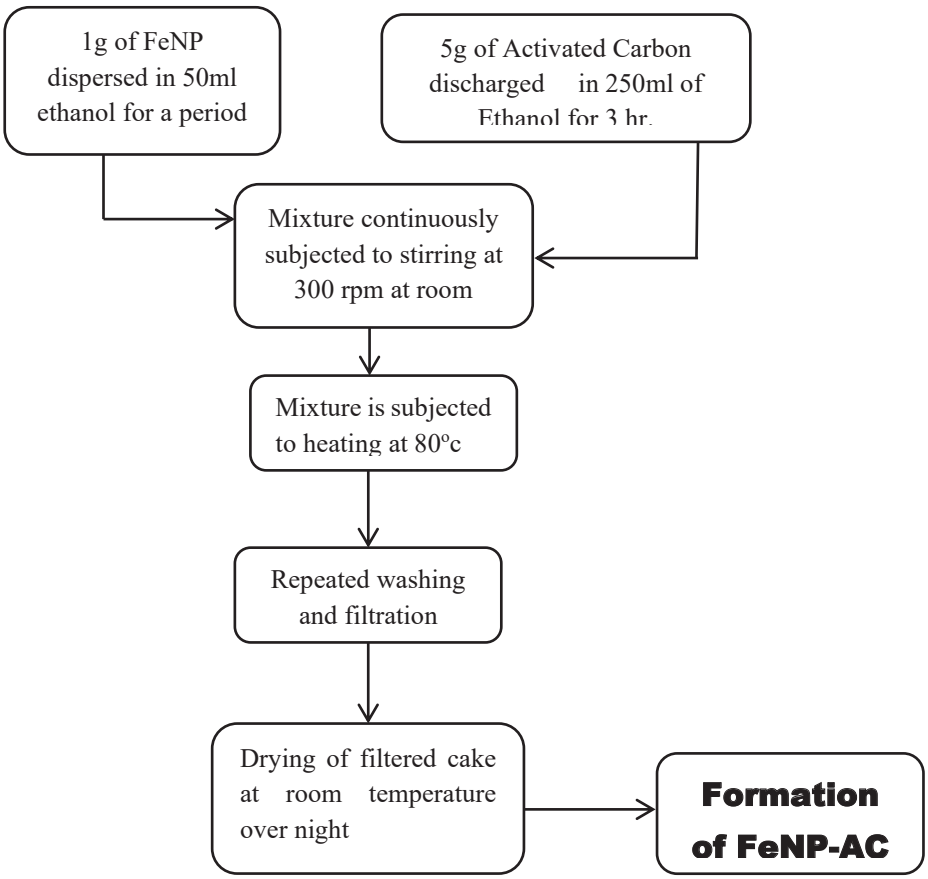

Fig. 6. Flow Diagram

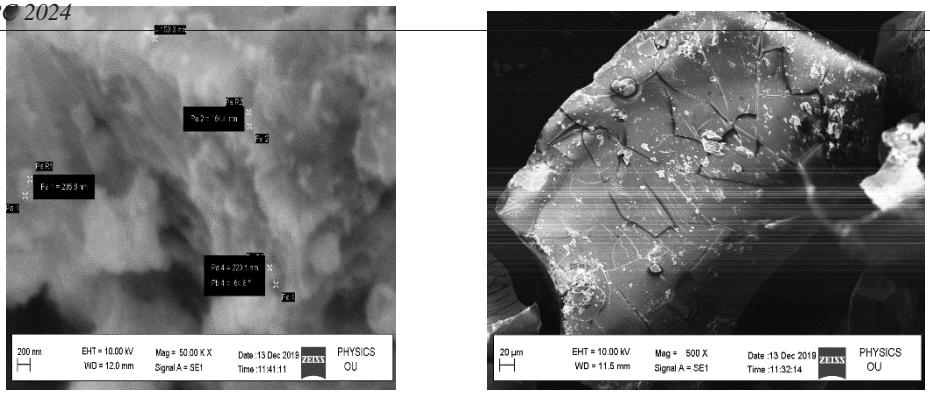

Fig. 7. Image of AP-Fe-ACNps

2.7 Characterization of AP-Fe-ACNps

Crystal violet sample was purchased from a chemical laboratory. This Crystal violet was diluted with distilled water and treated as crystal violet solution. From this solution crystal

2.7.1 Screening of extract using SEM :

Scanning Electron Microscope image shown in fig 3.7.1(a) magnificently projects the minute descriptional structures and varying sizes of AP-Fe-ACNps. It accommodates high-level resolution and stabilized probe currents for optimal images. Thus the generated nanoparticles fall under the range of 159.3 to205.6 nm.

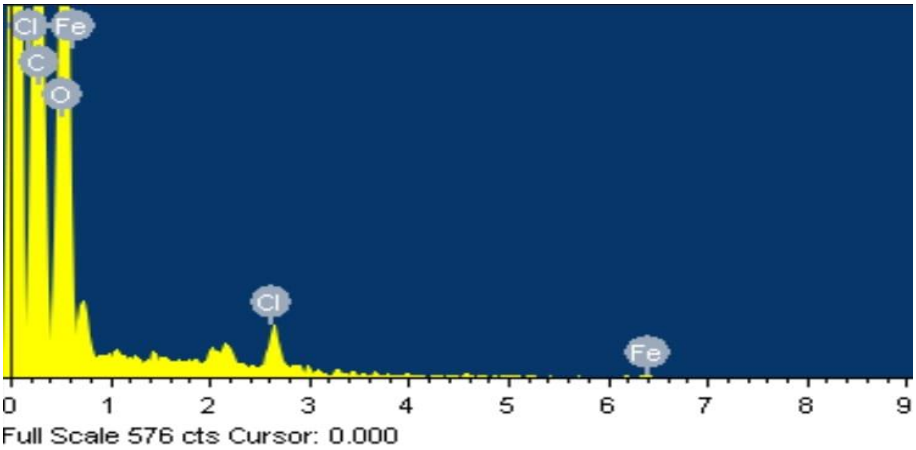

Fig. 8. Graphical representation of SEM AP-Fe-ACNps

2.7.2 X-Ray Diffraction (Analytics):

The rhetoric peak values for the figure-3.7.2 indicates the visible formation of hexagonal wurtzite structure . The notated peak positions at 2θ values of AP-Fe-ACNps are 5.74^0, 10.92^0, 17.94^0, 22.31^0, 28.52^0, 30.52^0. The XRD for AP-Fe-ACNps are shown in the below figure.

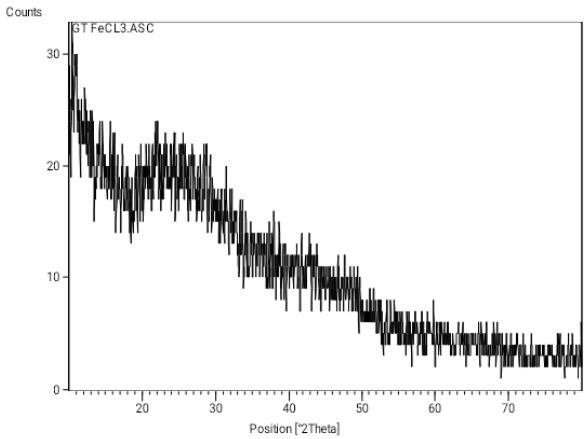

Fig. 9. XRD pattern AP-Fe-ACNps

3 Results And Discussion

The effects of contact time, dosage, solution pH, initial concentration, and solution temperature were investigated in order to maximize the percentage of removed crystal violet from the prepared crystal violet solution.

3.1 Charecterization of AP-Fe-ACNps

3.1.1 Fourier Transform Infra-Red Spectroscopy (FTIR) :

FTIR spectrum of Pure AP-Fe-ACNps is presented in Fig-4.4 . The peaks at different points represent different functional groups. Most functional groups include carboxylic, hydroxide and C=C groups. The peaks at 2450cm^{-1}, 2500cm^{-1}, for AP-Fe-ACNps before and after FTIR which may assigned to the OH groups, CH_2 group, C=O stretching, NO_2 aromatic nitro compound, C-O stretching, C-N stretching, CH bending vibrations respectively.

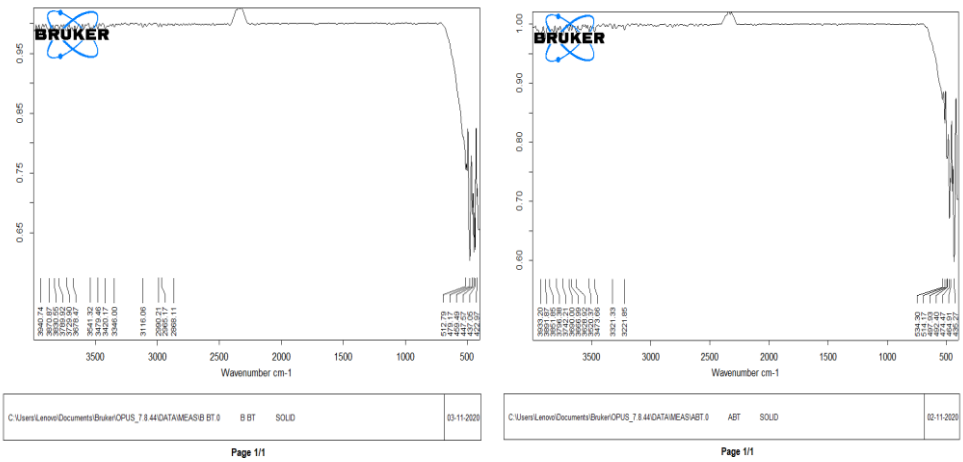

Fig. 10. FTIR before and after analysis of AP-Fe-ACNps

3.2 Experimental Parameters:

Using AP-Fe-Nps as an adsorbent, experimental data is produced in a batch mode of operation to investigate the impact of different parameters on the removal of Crystal violet from the aqueous solution (made in the laboratory). Experimental analysis is used to first determine how different parameters affect Crystal Violet adsorption, and theoretical justification of the findings using graphical analysis is then tried. The current investigation involves a number of experimental runs. The parameters examined are:

- Contact Time (t, minutes)
- Adsorbent Dosage (W, g/L)
- pH of the solution
- Initial Concentration of the solution (C_i, mg/L)
- Temperature (T,K)

3.2.1 Effect of Contact Time (t):

The graph displays the time course profiles of 1, 5, 10, 20, 30, 40, 50, 60, and 70 minutes for the adsorption of crystal violet solutions. The results of the crystal violet adsorption onto utilized AP-Fe-ACNps demonstrated that an equilibrium adsorption required 60 minutes of contact time, and that an additional 60 minutes of contact time did not significantly alter the dye's concentration. Therefore, the equilibrium values, qe (mg/g) and Ce (mg/L), are determined by measuring the dye uptake and remaining dye concentration after 60 minutes. The contact period for this AP-Fe-ACNps adsorbent has been set at 60 minutes, which is the equilibrium time, enabling further experiments on adsorption with other parameters. The percentage reduction is computed in this way:

$$\% \text{ Removal} = (C_i - C_t) \times 100 / C_0 \quad (1)$$

$$\text{Dye uptake, } q = (C_i - C_t) / W \quad (2)$$

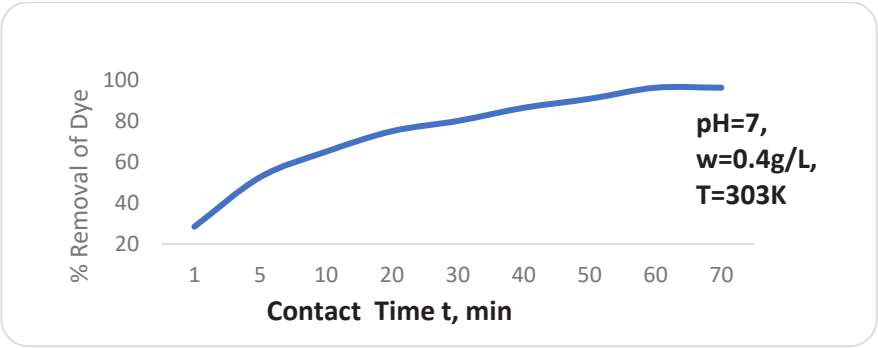

Graph. 1. Contact time for adsorption of crystal violet using AP-Fe-ACNps

3.2.2 Effect of adsorbent dosage (W):

While holding the other variables constant, the adsorbent dosage is changed from 0.1 to 0.5 g in order to investigate the impact of the dosage on the removal of crystal violet. Contact time is 60 minutes. The percent dye removal increases as the adsorbent dosage increases, as seen in Graph 4.2. For a 20 ppm dye solution, the percentage removal rose from 86.4% to 96.2% for AP-Fe-ACNps. The significant number of sorption sites and increased surface area

seen with an increase in adsorbent dosage from 0.1 to 0.5 g can be attributed to the increase in Crystal violet removal.

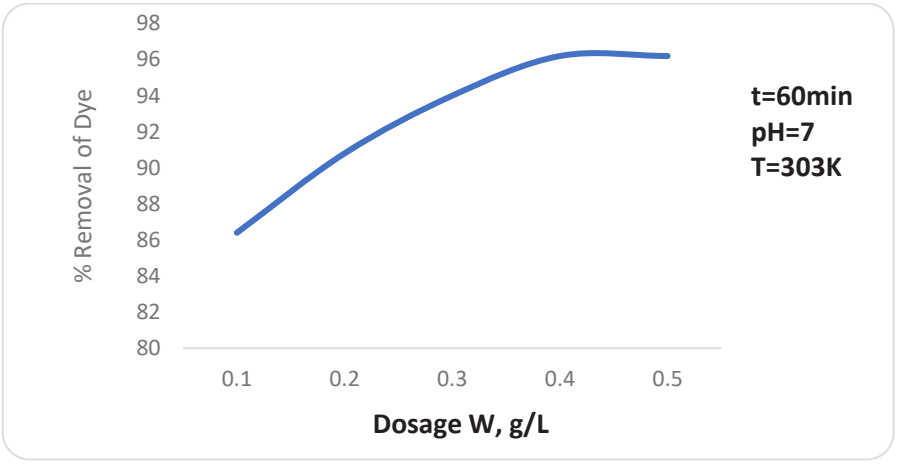

Graph. 2. Effect of Dosage for adsorption of crystal violet using AP-Fe-ACNps

3.2.3 Effect of solution pH:

One of the most crucial elements influencing the adsorption process is the initial pH. The impact of starting pH on crystal violet adsorption utilizing AP-Fe-ACNps is depicted in Graph 4.3. From pH 5 to pH 7, the percentage dye adsorption increased, and from there, the values fell as pH climbed to pH 9. Thus, 7 was determined to be the ideal pH.

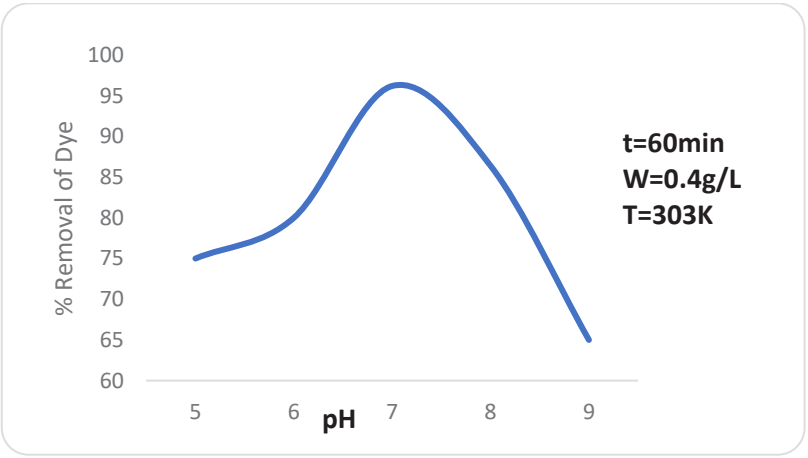

Graph. 3. Effect of pH for adsorption of crystal violet using AP-Fe-ACNps

3.2.4 Effect of initial concentration of aqueous dye solution:

Graph 4 shows the fluctuation of dye uptake and elimination percentage with initial concentration. Based on the graph, it was found that when the initial dye concentration was increased, the dye uptake increased and the proportion of dye removed has dropped.

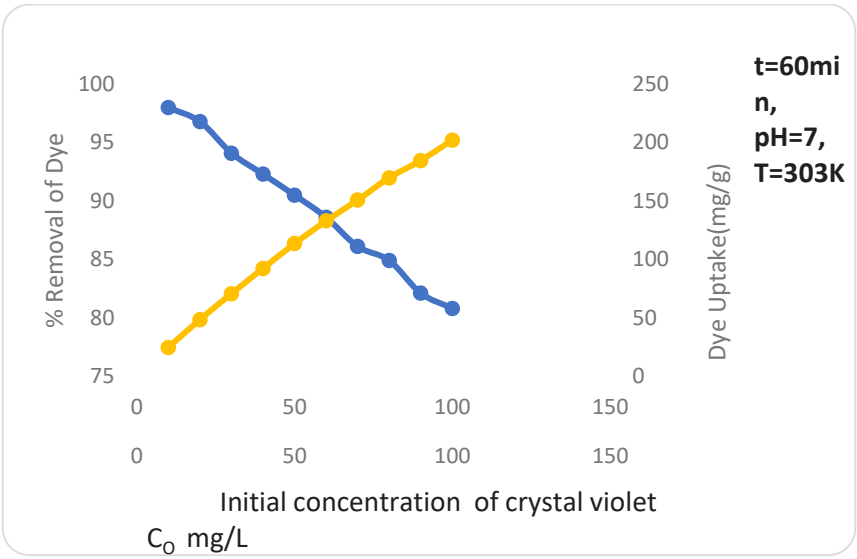

Graph. 4. Initial concentration for adsorption of crystal violet using AP-Fe-ACNps

3.2.5 Effect of Temperature (K):

The adsorption capability of AP-Fe-ACNps at various temperatures for the adsorption of crystal violet decreased as the temperature rose. Four constant temperatures—303, 308, 313, and 318 K—were used in batch studies to examine the impact of temperature. As can be seen in Graph-4.5, the percentage elimination increased with temperature, going from 98.0% to 99.2% mg/g for the initial concentration of 20 mg/L. This suggests that the nature of the adsorption process is endothermic.

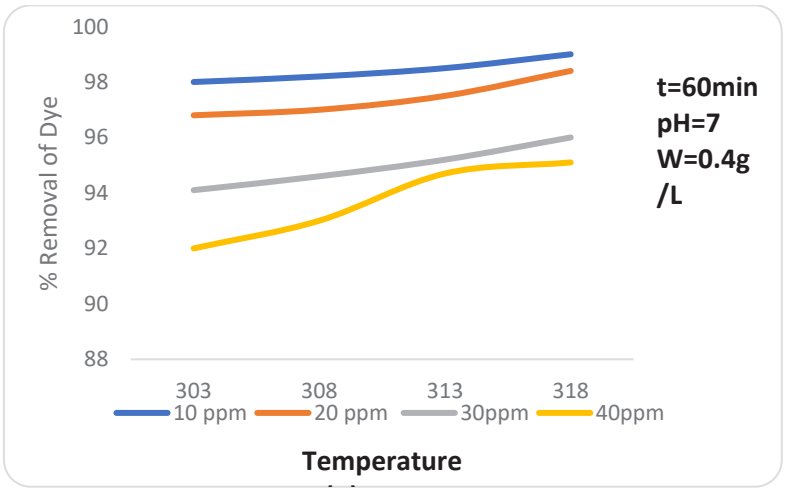

Graph. 5. Effect of Temperature for adsorption of crystal violet using AP-Fe-ACNps

3.3 Adsorption Kinetics:

3.3.1 Pseudo-first order kinetic model:

$$\ln(q_e-q)= -K_1t+\ln (q_e) \quad (3)$$

A plot is drawn between $\ln(q_e-q)$ and t.
Slope K_1 (min^{-1}) =0.045
Intercept $\ln(q_e)$ = 3.376
R^2 =0.982

The equation obtained: $\ln(q_e-q)= -0.045t+3.376$ (4)

From intercept q_e(calc) mg/g = 29.2
Equilibrium adsorption capacity q_e(exp) mg/g = 48.4

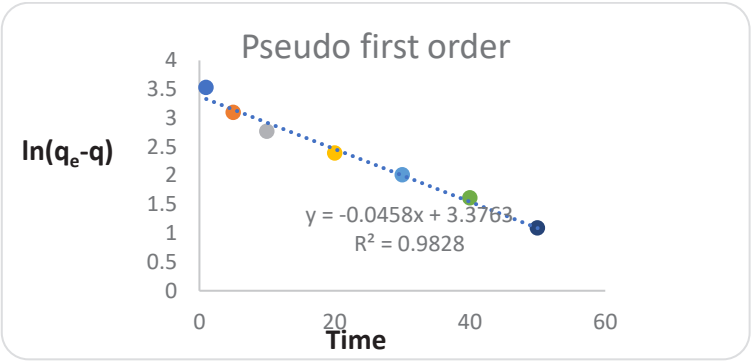

Graph. 6. Pseudo first order kinetics for adsorption of crystal violet using AP-Fe-Nps

3.3.2 Pseudo-second order kinetic model:

$$t/q = t/qe + 1/K2qe2 \quad (5)$$

intercept 1/K2qe2 = 0.084
R2 = 0.984

The equation obtained: $t/q = 0.021t + 0.084$ (6)

From intercept qe(calc)mg/g = 47.6
Equilibrium adsorption capacity q_e(exp) mg/g = 48.4

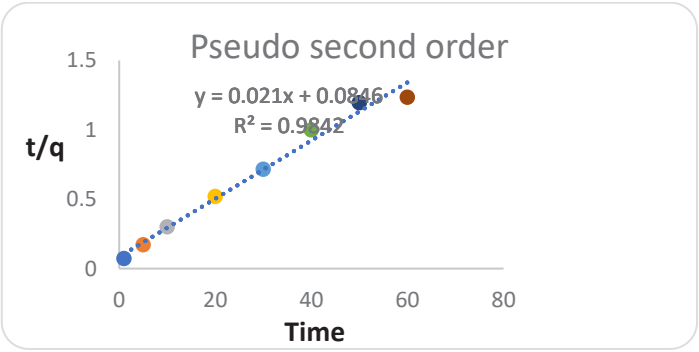

Graph. 7. Pseudo second order Kinetics for adsorption of crystal violet using AP-Fe-ACNps

3.3.3 Elovich Model

$$q_t = \frac{1}{\beta} ln(\alpha\beta) + \frac{1}{\beta} lnt \quad (7)$$

A plot is drawn between q_t and lnt
Slope $1/\beta = 7.233$
Intercept $\frac{1}{\beta} ln(\alpha\beta) = 17.19$
$R^2 = 0.957$

The equation obtained: $q_t = 7.233\ln(t) + 17.19$ (8)

From slope & intercept
Desorption constant $\beta = 0.138$g/mg
Initial rate constant $\alpha = 77.6$ mg/g.min

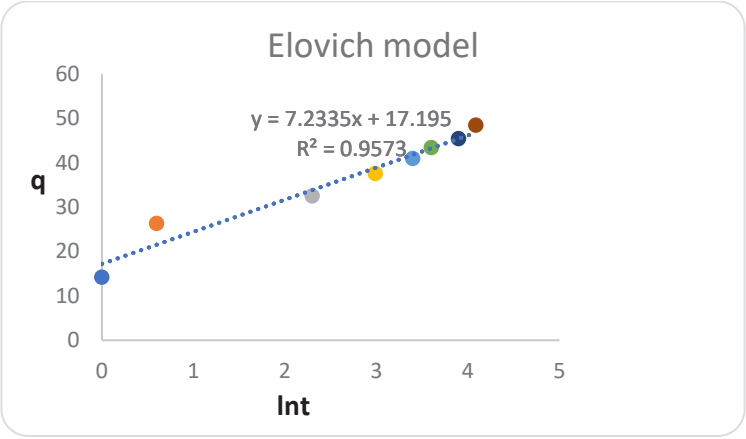

Graph. 8. Elovich model kinetics for the adsorption of crystal violet using AP-Fe-ACNps

3.4 Adsorption Isotherms:

3.4.1 Langmuir Isotherms:

$$\frac{C_e}{q_e} = \frac{1}{q_{max} kL} + \frac{1}{q_{max}} C_e \quad (9)$$

A graph is drawn between C_e/q_e and C_e

Slope $\frac{1}{q_{max}} = 0.004$

Intercept $\frac{1}{q_{max} kL} = 0.016$

$R^2 = 0.984$

The equation obtained: $\frac{C_e}{q_e} = 0.004\ C_e + 0.016$ (10)

From slope & intercept,

Langmuir constant i.e max. adsorption capacity q_{max} = 240mg/g
Adsorption intensity K_L = 0.25L/mg
Separation factor $R_L = 1/1+K_LC_o$
R_L values obtained were in between 0.03-0.2

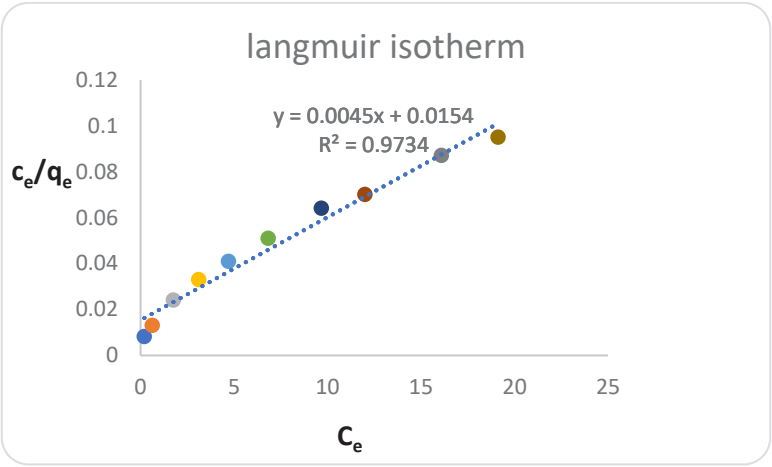

Graph. 9. Langmuir Isotherm for adsorption of crystal violet AP-Fe-ACNps

3.4.2 Freundlich Isotherm:

$$\log(q_e) = n \log(c_e) + \log K_F \quad (11)$$

A graph is drawn between $\log(q_e)$ and $\log(C_e)$
Slope n = 0.471
Intercept $\log K_F$ = 1.711
R^2 =0.992

The equation obtained: $\log(q_e) = 0.471\log(C_e) + 1.711$ (12)

From intercept, Freundlich constant $K_F(mg/g)/(mg/L)^n$ = 51.40

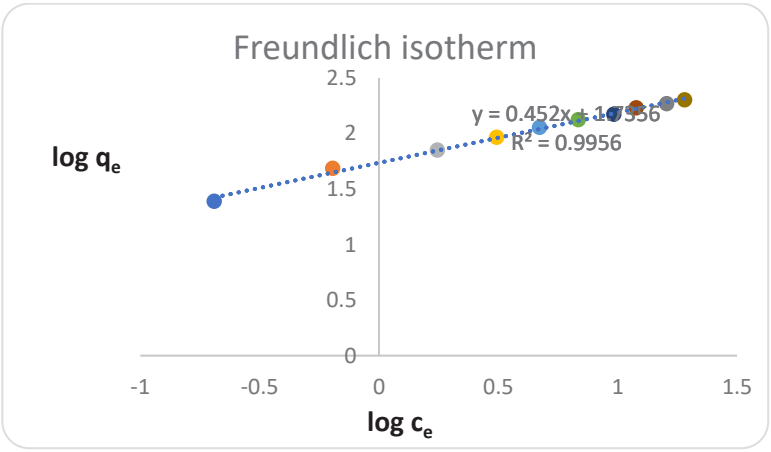

Graph. 10. Freundlich isotherm for adsorption of crystal violet using AP-Fe-ACNps

3.5 Thermodynamic studies:

Equilibrium constants that vary with temperature can be used in the estimation of thermodynamic parameters such as entropy change (ΔS^0), free energy change (ΔG^0), and enthalpy change (ΔH^0). The following formula provides the sorption reaction's free energy change:

$$\Delta G^o = -RT \ln K_a \quad (13)$$

Where,
ΔG^o is the standard free energy change, KJ/mol.
R is the universal gas constant. 8.314 $Jmol^{-1}K^{-1}$ and
T is the absolute temperature, Deg K.
The degree of spontaneity of the adsorption process is indicated by the free energy change, and a negative value indicates more energetically advantageous adsorption. The enthalpy change of adsorption as a function of temperature can be used to express the equilibrium constant as follows:

$$\frac{d \ln K_a}{dT} = \frac{\Delta H^0}{RT^2} \quad (14)$$

The sign of ΔH^0 determines the temperature's effect on the equilibrium constant K_a, as per Eq. (23). Therefore, a shift to the left in the adsorption equilibrium is implied when ΔH^0 is positive, meaning that an increase in temperature (T) results in an increase in K_a when the adsorption is endothermic. Conversely, when ΔH^0 is positive, meaning that an increase in temperature (T) results in a increase in K_a when the adsorption is endothermic. In general, ΔG^0 ranges from -20 KJ/mol to 0 KJ/mol for physisorption and from -80 KJ/mol to -400 KJ/mol for chemisorption.
The integrated form of Eq. (23) becomes

$$\ln K_a = \frac{-\Delta H^0}{RT} + \Delta S \quad (15)$$

Eq (24) can be rearranged to

$$-RT \ln K_a = \Delta H^o - TR\,\Delta S \quad (16)$$

Where ΔS^o is, the change with temperature o the free energy change with temperature and the equilibrium constant can be represented as follows:

$$\Delta G^o = \Delta H^o - T\Delta S^o \quad (17)$$

$$\ln K_a = \frac{-\Delta H^o}{RT} + \frac{\Delta S^o}{R} \quad (18)$$

Equation (27) makes it evident that the two components of the adsorption process which are enthalpic change and entropic change which determine whether the reaction is spontaneous. Graph 4.11 displays the ΔG^0, ΔH^0, and ΔS^0 values of crystal violet dye ions at various temperatures 303K-318K.

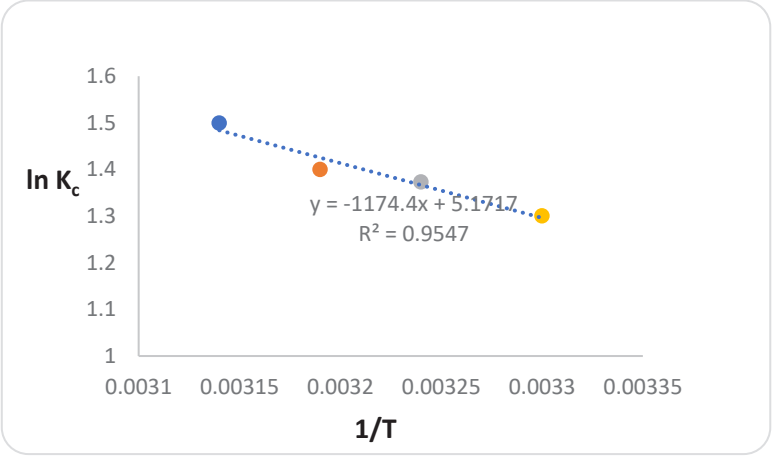

Graph. 11. Van't Hoffs thermodynamic plot for adsorption of crystal violet using AP-Fe-ACNps

4 Conclusion

Using Albizia procera leaves, an easy, quick, and environmental friendly method is employed for the synthesis of AC-FeNPs rather than other alternative options for eliminating crystal violet stain, which is used in pesticides as a coloring agent and disinfectant.Using AP-Fe-ACNps as an adsorbent, experimental data was collected for the removal of crystal violet dye. The experimental study leads to the following results. Temperature, adsorbent dosage, pH, initial dye concentration, contact time, and so on all had a significant impact on the adsorption performance. An increase in duration of contact time led to an increase in the percentage of Crystal Violet adsorption. An increase in the adsorbent dosage resulted in a drop in equilibrium uptake and an increase in percentage adsorption. Plotting pH against percentage of dye removal revealed that substantial adsorption occurred at a pH of 7. An increase in the starting dye concentration resulted in a drop in the percentage of Crystal Violet adsorption and a significant rise in dye uptake. A rise in temperature was correlated with an increase in the proportion of Crystal Violet adsorption. Thus, this suggests that physisorption is taking place. Albizia procera was discovered to be a novel source of adsorbent for the removal of dye from effluent waste that contained low concentrations of dyes according to the current investigation.The experimental data for AP-Fe-ACNps was best adjusted by the Freundlich and Langumir isotherm models for Crystal violet. The kinetics of Crystal Violet's adsorption on AP-Fe-ACNps is characterized using pseudo-second-order kinetics. The calculation of thermodynamic parameters, including changes in free energy, enthalpy, and entropy, leads to the conclusion that the adsorption process is endothermic in nature.

References

1. J. Yang, B. Hou, J. Wang, B. Tian, J. Bi, N. Wang, X. Li, X. Huang, Nanomaterials for the Removal of Heavy Metals from Wastewater, Nanomaterials. **9**(3),424 (2019)DOI:10.3390/nano9030424
2. H. J. Kumari, P. Krishnamoorthy, T. K. Arumugam, S. Radhakrishnan, D. Vasudevan, An efficient removal of crystal violet dye form waste water by adsorption onto TLAC/chitosan composite: A novel cost adsorbent, International Journal of Biological Macromolecules. **96**, 324-333 (2017) https://doi.org/10.1016/j.ijbiomac.2016.11.077

3. I. H. Singh, A. Singh, H. Singh, Green synthesis of nanoparticles and its potential application, Biotechnol Lett. **38**, 545–560 (2016)
4. S. Saif, A. Tahir, Y. Chen, Green Synthesis of Iron Nanoparticles and Their Environmental Applications and Implications, Nanomaterials. **6**(11**)**, 209 (2016) https://doi.org/10.3390/nano6110209
5. C. P. Devatha, A. K. Thalla, S. Y. Katte, Green synthesis of iron nanoparticles using different leaf extracts for treatment of domestic waste water, Journal of Cleaner Production. **139**, 1425-1435 (2016) https://doi.org/10.1016/j.jclepro.2016.09.019
6. C. Muthukumaran, V. M. Sivakumar, M. Thirumarimurugan, Adsorption isotherms and kinetic studies of crystal violet dye removal from aqueous solution using surfactant modified magnetic nanoadsorbent, Journal of the Taiwan Institute of Chemical Engineers. **63**, 354-362 (2016) https://doi.org/10.1016/j.jtice.2016.03.034
7. S. Hadi, R. K. Ahmad, N. Reza, Adsorption of malachite green and crystal violet cationic dyes from aqueous solution using pumice stone as a low-cost adsorbent: kinetic, equilibrium and thermodynamic studies, Desalination and Water Treatment. **57** (27): 12822-12831 (2016) https://doi.org/10.1080/19443994.2015.1054315
8. A. Kavitha, G. Sai Pooja, M. Kaaviyavarshini, Colour Removal of textile dyeing effluent using Low Cost adsorbents, International Journal of Engineering Research and General Science. **4**(2), 732-748 (2016)
9. P. Balaji, Removal of Colour from Textile Effluent using Natural Adsorbent (Calotropis Gingantea), International Journal of Innovations in Engineering and Technology. **5**(4), 2319-1058 (2015)
10. L. Giraldo, A. Erto, J. C. M. Pirajᾶn, Magnetite nanoparticles for removal of heavy metals from aqueous solutions: synthesis and characterization, Adsorption. **19**, 465–474 (2013) https://doi.org/10.1007/s10450-012-9468-1
11. T. Shahwana, S. A. Sirriaha, M. Nairat, E. Boyac, A.E. Eroglu, T.B. Scott, K.R. Hallamc, Green synthesis of iron nanoparticles and their application as a Fenton-like catalyst for the degradation of aqueous cationic and anionic dyes, Chemical Engineering Journal. **172** (1), 258-266 (2011) https://doi.org/10.1016/j.cej.2011.05.103
12. K. P. Singh, S. Gupta, A. K. Singh, S. Sinha, Optimizing adsorption of crystal violet from water by magnetic nanocomposite using response surface modeling approach, Journal of Hazardous Materials. 186 (2–3), 1462-1473 (2011) https://doi.org/10.1016/j.jhazmat.2010.12.032
13. Y. M. Ahmed, A. A. Mamun, M. SA, M. A. F. R. A. Khatib, A.T. Jameel, M. A. Alsaadi, Study of Pb Adsorption by Carbon Nanofibers grown on Powdered Activated Carbon, Journal of Applied Science. **10**, 1983-1986 (2010)
14. M. M. Sundaram, N. Kannan, J. Rejinis, Adsorption Kinetics of Nile Blue A, safranine and ethyl violet on commercial activated carbon –A comparative study, Indian Journal of Environmental protection. **30**(1), 1-9 (2010)
15. N. Kannan, S. Murugavel, Kinetic studies on the removal of various dyes by adsorption of fly ash and commercial activated carbon, Indian Journal of Environmental protection. **30**(1), 74-80 (2010)
16. M. Alok, M. Jyoti, A. Malviya, D. Kaur, V.K. Gupta, Adsorption of hazardous dye crystal violet from wastewater by waste materials, Journal of Colloid and Interface Science. **343**, 463–473 (2010) https://doi.org/10.1016/j.jcis.2009.11.060